

If we substitute (A-5) into (A-3) and make use of (IV-3), we have

$$\left(1 + \frac{Z_1}{Z_{pv}}\right) = \frac{\sum_{j=0}^{y+1} b(y+1, j)K^j(s)}{\sum_{j=0}^y b(y, j)K^j(s)} \quad (\text{A-6})$$

and

$$V_\beta = \frac{V_{in}}{\prod_{y=n-\beta}^{n-1} \frac{\sum_{j=0}^{y+1} b(y+1, j)K^j(s)}{\sum_{j=0}^y b(y, j)K^j(s)}} \quad (\text{A-7})$$

After reduction of the numerator and denominator terms (A-7) becomes

$$V_\beta = \frac{\sum_{j=0}^{n-\beta} b(n-\beta, j)K^j(s)}{\sum_{j=0}^n b(n, j)K^j(s)} V_{in} \quad (\text{A-8})$$

The (A-8) coincides with the (IV-2).

## APPENDIX II

### Fibonacci Numbers

Fibonacci numbers can be obtained from the following simplest recursive formula:

$$F_n = F_{n-1} + F_{n-2} \quad (n \geq 2)$$

with the initial conditions

$$F_0 = 0, F_1 = 1$$

$$\begin{array}{ccccccccccccccc} F_0 & F_1 & F_2 & F_3 & F_4 & F_5 & F_6 & F_7 & F_8 & F_9 & F_{10} & F_{11} & \cdots \\ 0 & 1 & 1 & 2 & 3 & 5 & 8 & 13 & 21 & 34 & 55 & 89 & \cdots \end{array}$$

Formulas to generate them, however, are numerous and can be found in [10].

## ACKNOWLEDGMENT

The authors would like to thank Prof. Unbehauen and all the reviewers for their advice.

## REFERENCES

- [1] W. A. Blackwell, *Mathematical Modelling of Physical Networks*. New York: Macmillan, 1968.
- [2] G. C. Temes and S. K. Mitra, *Modern Filter Theory and Design*. New York: Wiley, 1973.
- [3] M. A. Maher, S. DeWeerth, M. Mahowald and C. Mead, "Implementing neural architectures using analog VLSI circuits," *IEEE Trans. Circuits Syst.*, vol. 36, no. 5, pp. 643-652, May 1989.

- [4] R. Goyal, Ed., *Monolithic Microwave Integrated Circuits: Technology and Design*. Norwood, MA: Artech House, 1989.
- [5] M. N. S. Swamy and B. B. Bhattacharyya, "A study of recurrent ladders using the polynomials defined by Morgan-Voice," *IEEE Trans. Circuit Theory*, vol. CT-14, pp. 260-264, Sept. 1967.
- [6] G. Ferri, M. Faccio, and A. D'Amico, "A new numerical triangle showing links with Fibonacci numbers," to be published in *The Fibonacci Quarterly*.
- [7] —, "Fibonacci numbers and ladder network impedance," to be published in *The Fibonacci Quarterly*.
- [8] A. D'Amico, M. Faccio, and G. Ferri, *Ladder Network Transfer Function and Thevenin's Model Determination*, Research Reports of Microelectronics and Telecommunication 1-89, Dep. Elec. Eng., Univ. di L'Aquila, Jan. 1989.
- [9] M. Bicknell, "A primer on the Pell sequence and related sequences," *The Fibonacci Quarterly*, vol. 13, pp. 345-349, 1975.
- [10] P. Filippini, *I Numeri di Fibonacci*. Sistemi di Telecomunicazioni, pp. 40-50, Dec. 1989.
- [11] A. M. Morgan-Voice, "Ladder-network analysis using Fibonacci numbers," *IRE Trans. Circuit Theory*, vol. 6, pp. 321-322, Sept. 1959.
- [12] J. Lahr, "Fibonacci and Lucas numbers and the Morgan-Voice polynomials in ladder networks and in electric line theory," in *Fibonacci Numbers and Their Appl.*, A. N. Philippou, G. E. Bergum, and A. F. Horadam, Eds. Dordrecht: D. Reidel, 1986.
- [13] C. A. Mead, *Analog VLSI and Neural System*. Reading, MA: Addison Wesley, 1989.

## Exact Simulation of Feedback Circuit Parameters

Paul J. Hurst

**Abstract**—Techniques for finding the important parameters of a single-loop feedback circuit at the closed-loop dc operating point are presented. The main advantage of these techniques is that they allow exact computer simulation of feedback parameters with a circuit simulator such as SPICE. By maintaining the closed-loop dc bias point in all test circuits, the small-signal models for all nonlinear elements are computed correctly by the circuit simulator. The methods presented for simulating loop transmission are particularly valuable since they can be used to accurately determine gain and phase margin using frequency-domain analysis, which is faster and more efficient than simulating step response via transient analysis. The equations behind the two methods for calculating loop transmission are presented as background. Examples are included to demonstrate the techniques.

## I. INTRODUCTION

Feedback is present in virtually all analog circuits. Initial design of feedback circuits requires some simplifying assumptions, such as large low-frequency loop gain, negligible forward transmission through the feedback circuit, and negligible reverse transmission through the forward amplifier. Such approximations simplify the design equations [1]-[3]. The properties of feedback circuits are either described in terms of the return

Manuscript received June 19, 1990; revised March 1, 1991. This work was supported in part by the UC MICRO Program, cosponsored by Precision Monolithics, Inc., Rockwell International, and Silicon Systems, Inc., and in part by the National Science Foundation under Grant MIP-8910288. This paper was recommended by Associated Editor R. K. Hester.

The author is with the Solid-State Circuits Research Laboratory, Department of Electrical Engineering and Computer Science, University of California, Davis, CA 95616.  
IEEE Log Number 9102889.

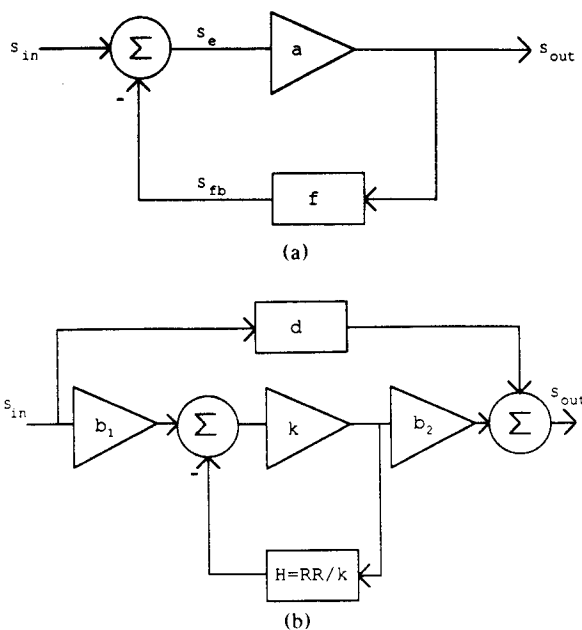


Fig. 1. (a) Ideal feedback circuit block diagram corresponding to (3).  $S$  may be a voltage or a current. (b) Signal-flow diagram corresponding to (2).

ratio of a dependent source, as was done in the early feedback text by Bode [4], or in terms of the classical feedback block diagram of Fig. 1(a) with unilateral forward gain  $a$ , unilateral reverse transmission factor  $f$ , and loop gain  $af$ . (The term *loop gain* will refer to  $af$  of Fig. 1(a) in this paper.<sup>1</sup>) Return ratio ( $RR$ ) and loop gain  $af$  of Fig. 1(a) are two different quantities; both present useful information about the loop properties of a given feedback circuit. Each has an associated set of equations that can be applied to find the closed-loop parameters [1]–[6].

Procedures that allow the important feedback parameters to be found exactly while maintaining the closed-loop dc operating point are presented below. One technique finds  $RR$ ; the other finds  $f$  and  $af$ . The techniques are applicable to *single-loop* feedback amplifiers [4], [5], [7], which include most op-amp feedback circuits and many others. A single-loop feedback circuit is one in which there is one unique signal path that traverses the feedback loop.

In the next section, the gain equations incorporating return ratio and loop gain are reviewed, and an example is presented to show that return ratio and loop gain can be quite different. Then techniques for simulating return ratio and loop gain at the closed-loop dc operating point are presented. For clarity, the shunt-shunt feedback circuit in Fig. 2 is used in the discussions below, but the techniques are completely general and can be applied to all four types of feedback circuits. Some examples are followed by a section that shows that return ratio is the loop gain of an appropriately defined transfer function. The IEEE conventions for dc and ac signals are used throughout the paper; a capitalized signal variable with a capitalized subscript indicates a dc quantity (e.g.,  $I_{IN}$ ), a lower-case signal variable with lower-case subscript indicates an ac quantity (e.g.,  $i_{in}$ ), and a lower-case signal variable with upper-case subscript indicates a total—ac plus dc—quantity (e.g.,  $i_{IN}$ ).

<sup>1</sup> Many tests use the terms “return ratio” and “loop gain” interchangeably. However, as will be shown, the two are different.

## II. BACKGROUND AND EQUATIONS

### 2.1. Feedback Circuit Analysis Method 1—Bode's Return Ratio

In the original feedback text by Bode [4] and in other texts [5]–[7], the closed-loop properties of feedback circuits are described in terms of the *return ratio* of a dependent source in an active device. The return ratio for a controlled source can be found by 1) setting all independent sources to zero, 2) selecting a dependent source, 3) breaking the connection between that source and the rest of the circuit, 4) driving the circuit at the break with an independent source of the same type with value  $s_t$ , and 5) finding the output  $s_r$  from the dependent source. Then the return ratio for that dependent source is  $RR = -s_r/s_t$ . ( $S$  may be a current or a voltage.)

The formulas presented in this paper are valid for single-loop feedback amplifiers [4], [5], [7]. For a single-loop amplifier with multiple dependent sources, the return ratios for all dependent sources in the active devices are the same, or, equivalently, setting any dependent source to zero causes the return ratio for all other dependent sources to go to zero.

The exact formula for the closed-loop gain of a feedback amplifier as it relates to the return ratio of a dependent source in an active device is [4]

$$A_{cl} = \frac{b}{1 + RR} + d. \quad (1)$$

Formulas for  $b$  and  $d$  will now be given. Call the value of the control parameter  $k$ . (In the case of a bipolar transistor's controlled source  $i_c = g_m v_{be}$ ,  $k = g_m$ , and  $v_{be}$  is the controlling signal.) Then the calculation of  $b$  breaks into three parts:  $b = b_1 \cdot k \cdot b_2$  where

- $b_1$  = transfer function from the input to the control signal evaluated with  $k = 0$ ,
- $b_2$  = transfer function from the dependent source to the output evaluated with the input source set to zero, and
- $d$  = transfer function from input to output evaluated with  $k = 0$ .

From its definition, the return ratio is of the form  $RR = k \cdot H$ , where  $H$  is the transfer function from  $s_t$  to the controlling signal. Therefore, (1) can be rewritten as

$$A_{cl} = b_1 \cdot \frac{k}{1 + RR} \cdot b_2 + d = b_1 \cdot \frac{k}{1 + kH} \cdot b_2 + d. \quad (2)$$

A block diagram corresponding to (2) is shown in Fig. 1(b). Often  $d$  can be neglected for low-frequency analysis, but this direct feedthrough term can be important at high frequencies.  $RR = k \cdot H$  is the gain around the loop in Fig. 1(b), which is not necessarily equal to the gain  $af$  around the loop in Fig. 1(a).

### 2.2. Feedback Circuit Analysis Method 2—Two-Port Analysis

Classical feedback analysis relates the closed-loop properties of feedback circuits to the open-loop properties of an appropriately defined forward amplifier  $a$ , the reverse transmission factor  $f$ , and the loop gain  $af$  [1]–[3], [8]. There are many advantages to using this analysis method.

- 1) The feedback circuit can be viewed as an implementation of the classical feedback block diagram (Fig. 1(a)).
- 2) Simple equations relate the open-loop and closed-loop properties of the feedback circuit, i.e.,  $Z_{out}$  and  $Z_{in}$  are modified by the factor  $(1 + af)$ .

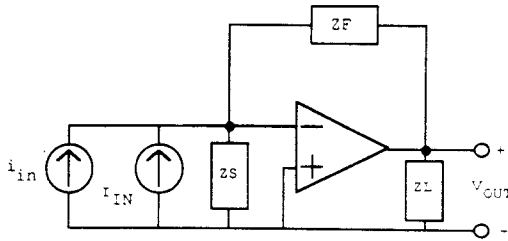


Fig. 2. Shunt-shunt feedback circuit to be analyzed. Resistor values are  $R_S = 500 \text{ k}\Omega$ ,  $R_F = 100 \text{ k}\Omega$ . Op-amp parameters:  $R_{in_a} = 1/y_{11a} = 1 \text{ M}\Omega$ ,  $R_{out_a} = 1/y_{22a} = 1 \text{ M}\Omega$ ,  $G_m = y_{21a} = 10 \text{ m}\Omega^{-1}$ ,  $y_{12a} = 0 \text{ }\Omega^{-1}$ .

### 3) The closed-loop gain expression

$$A_{cl} = \frac{a}{1 + af} \quad (3)$$

is in a "standard" form that allows well-known results from control theory to be used to predict closed-loop frequency response from  $af$  and  $a$  or  $f$ .

Manipulation of feedback circuits into the ideal feedback form of Fig. 1(a) is carried out through two-port analysis [1]–[3], [8]. The first step is identification of a feedback two-port and a forward amplifier two-port.<sup>2</sup> They are analyzed separately as two-ports, and the interconnection of these two two-ports is manipulated into ideal feedback form with one forward controlled source and one reverse controlled source. Once rearranged, this interconnection of two-ports agrees with Fig. 1(a) since the ideal forward amplifier and feedback network are unilateral.

An example of this procedure for the shunt-shunt feedback circuit in Fig. 2 is shown in Fig. 3. (For convenience here and in the majority of this paper, the shunt-shunt feedback configuration and the associated  $y$ -parameters are used in figures and examples. However, the methods are completely general and can be applied to all four feedback configurations.) The parameters  $a$ ,  $f$ , and  $af$  can be calculated from the redrawn two-port in Fig. 3(b):

$$f \triangleq \frac{i_{fb}}{v_o} = y_{12} = y_{12f} + y_{12a} \quad (4)$$

$$a \triangleq \frac{v_o}{i_e} = -\frac{y_{21}}{y_{11}y_{22}} = -\frac{y_{21a} + y_{21f}}{(y_{11a} + y_{11f}) \cdot (y_{22a} + y_{22f})} \quad (5)$$

(In this paper, the source admittance  $y_S$  and load admittance  $y_L$  are assumed to have been absorbed into  $y_{11a}$  and  $y_{22a}$ , respectively. Also, a  $y$ -parameter written as  $y_{ij}$  is a "total" parameter; that is,  $y_{ij} = y_{ija} + y_{ijf}$ .) The loop gain  $af$  is a crucial parameter of a feedback circuit. For the shunt-shunt feedback circuit example,

$$af = -\frac{y_{21}y_{12}}{y_{11}y_{22}} = -\frac{(y_{21a} + y_{21f}) \cdot (y_{12a} + y_{12f})}{(y_{11a} + y_{11f}) \cdot (y_{22a} + y_{22f})} \quad (6)$$

### 2.3. An Example Comparing RR and $af$

While either method can be used to analyze a feedback circuit, there are differences in the closed-loop formulas incorporating  $af$  and  $RR$ . In general,  $af$  is not the same as  $RR$ . Many popular texts argue intuitively that measuring the return ratio for a given dependent source is in some sense the same as

<sup>2</sup>Sometimes it is impossible to find such two-ports; examples are multi-loop feedback circuits such as fig. 8.28 of [1] or fig. 5.11 of [6].

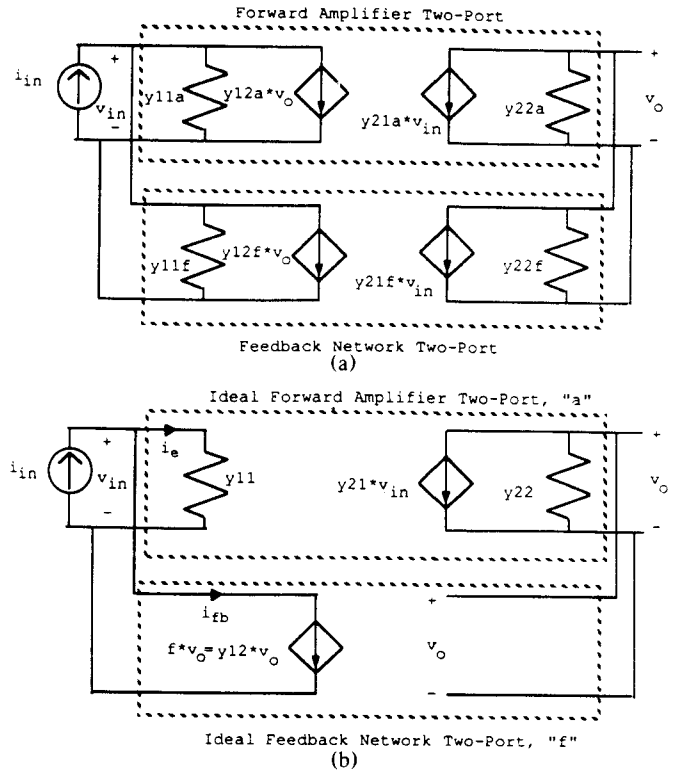


Fig. 3. (a) Small-signal two-ports for  $a$  and  $f$  networks for a shunt-shunt feedback circuit such as Fig. 2. (b) The ideal feedback form for the two-ports in (a) where  $y_{11} = y_{11f} + y_{11a}$ ,  $y_{12} = y_{12f} + y_{12a}$ ,  $y_{21} = y_{21f} + y_{21a}$ , and  $y_{22} = y_{22f} + y_{22a}$ .

breaking the loop in Fig. 1(a), and therefore,  $RR = af$  [1], [2], [4], [6], [9]. This is correct, however, only under certain specific conditions that are discussed in Section VI.

To clearly point out the potential for large differences between  $af$  and  $RR$ , the low-frequency loop gain and return ratio have been calculated for Fig. 2 using the element values in the figure caption. The loop gain for this shunt-shunt feedback circuit is

$$\begin{aligned} af &= -\frac{(y_{21a} + y_{21f}) \cdot (y_{12a} + y_{12f})}{(y_{11a} + y_{11f}) \cdot (y_{22a} + y_{22f})} \\ &= -\frac{\left(10 \text{ m}\Omega^{-1} - \frac{1}{100 \text{ k}\Omega}\right) \cdot \left(\frac{-1}{100 \text{ k}\Omega}\right)}{\left(\frac{1}{500 \text{ k}\Omega} + \frac{1}{1 \text{ M}\Omega} + \frac{1}{100 \text{ k}\Omega}\right) \cdot \left(\frac{1}{1 \text{ M}\Omega} + \frac{1}{100 \text{ k}\Omega}\right)} \\ &= 699. \end{aligned} \quad (7)$$

The  $RR$  is easily calculated by breaking the loop at the the op-amp's  $G_m$  generator:

$$\begin{aligned} RR &= G_m \cdot \frac{R_{out_a}}{R_S \parallel R_{in_a} + R_F + R_{out_a}} \cdot (R_S \parallel R_{in_a}) \\ &= 10 \text{ m}\Omega^{-1} \cdot \frac{1 \text{ M}\Omega}{500 \text{ k}\Omega \parallel 1 \text{ M}\Omega + 100 \text{ k}\Omega + 1 \text{ M}\Omega} \\ &\quad \cdot (500 \text{ k}\Omega \parallel 1 \text{ M}\Omega) = 2326. \end{aligned} \quad (8)$$

The results are significantly different and point out the importance of correctly finding  $RR$  or  $af$  and using the proper associated formulas when calculating closed-loop parameters. It should be noted that the usual text-book assumptions  $|y_{21f}| \ll$

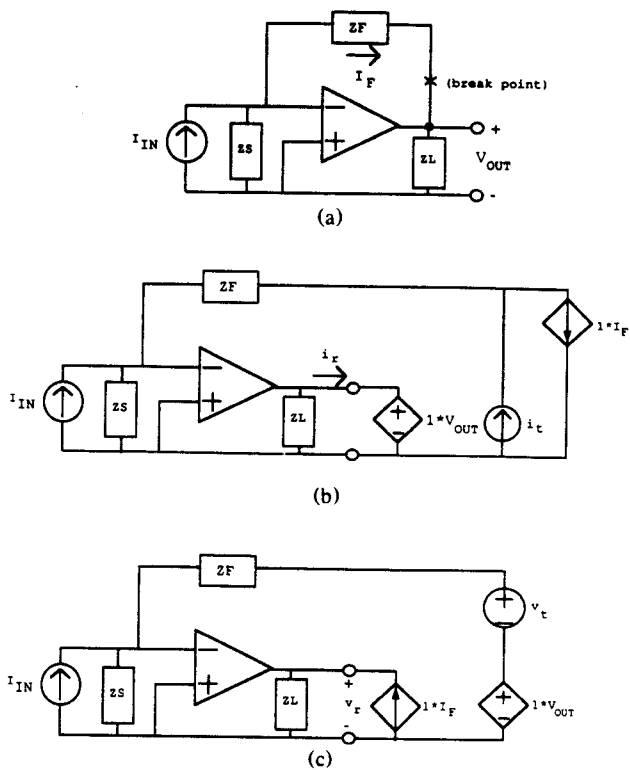


Fig. 4. Measurement of  $RR$  including controlled sources to maintain the correct dc bias: (a) Closed-loop dc reference circuit. (b) Measurement of  $RR_I$  at the closed-loop bias point. (c) Measurement of  $RR_V$  at the closed-loop bias point.

$|y_{21a}|$  and  $|y_{12a}| \ll |y_{12f}|$ , which are true in this example, are not sufficient to guarantee that  $RR = af$ .

### III. SPICE SIMULATION OF RETURN RATIO

In transistor circuits, the controlled sources and the controlling nodes are internal to the devices and hence are not accessible for return ratio computation. A technique that finds the return ratio by breaking the feedback loop at an arbitrary point and using a combination of generalized return ratios to measure the overall return ratio was presented in [10] as an extension of method four in [11]. The approach described there finds the return ratio for the controlled source(s) in the feedback amplifier by breaking the loop at an arbitrary point and computing both a current return ratio  $RR_I$  and a voltage return ratio  $RR_V$ .  $RR_I$  ( $RR_V$ ) is found by setting all independent sources in the linearized small-signal circuit to zero, breaking the loop, injecting a test current  $i_t$  (test voltage  $v_t$ ), and measuring the return current  $i_r$  (return voltage  $v_r$ ) flowing into a short circuit (appearing across an open circuit) at the other side of the break point. Then the total return ratio  $RR$  is given by

$$RR = \left[ \frac{1}{RR_I} + \frac{1}{RR_V} \right]^{-1} = - \left[ \frac{1}{\frac{i_r}{i_t}} + \frac{1}{\frac{v_r}{v_t}} \right]^{-1} \quad (9)$$

The dc operating point can be preserved during simulation of  $RR_I$  and  $RR_V$  as shown in Fig. 4. The closed-loop circuit in Fig. 4(a), with all ac sources set to zero, acts as a dc reference circuit. Controlled sources, controlled by dc voltages and currents in the reference circuit, are included in the  $RR_I$  and  $RR_V$  test circuits

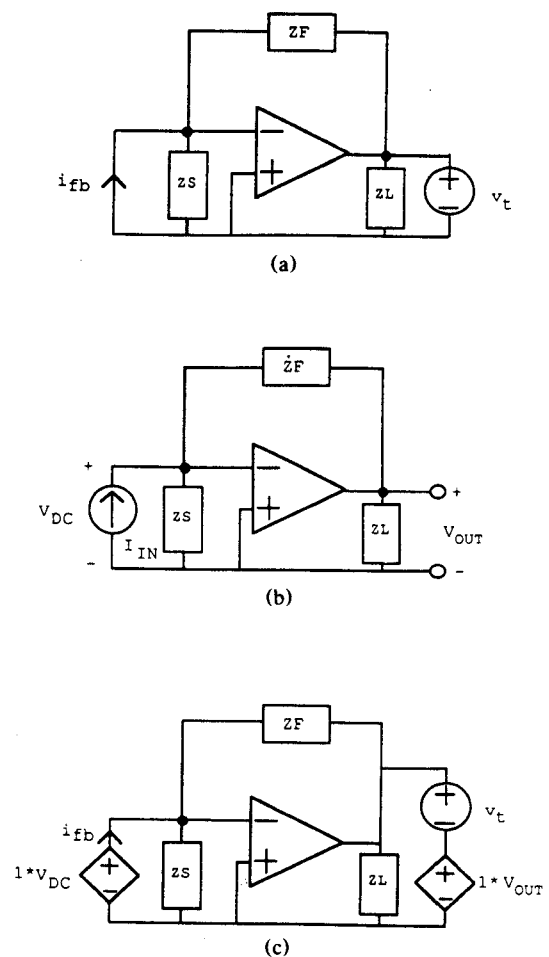


Fig. 5. Measurement of  $f$  for the circuit in Fig. 2. (a) Small-signal circuit concept. (b) dc reference circuit for (c). (c) Measurement of  $f$  at the closed-loop dc operating point.

at the breaks to replicate the closed-loop dc operating point. The advantage of maintaining the dc operating point is that all nonlinear elements in the feedback circuit, such as the transistors and junction capacitances, are properly biased; therefore, the circuit simulator automatically computes the correct small-signal models for the linear analysis.

### IV. SPICE SIMULATION OF TWO-PORT FEEDBACK PARAMETERS

If a feedback circuit can be modeled by properly interconnected  $a$  and  $f$  two-ports (Fig. 3(a)), then a single two-port analysis can be performed on the entire closed-loop feedback circuit and the resulting two-port parameters will be  $y_{11} = y_{11f} + y_{11a}$ ,  $y_{12} = y_{12f} + y_{12a}$ ,  $y_{21} = y_{21f} + y_{21a}$ , and  $y_{22} = y_{22f} + y_{22a}$ , which are the four parameters of the ideal feedback two-port shown in Fig. 3(b). This observation is the basis of the following simulation procedures.

#### 4.1. Simulating $f$

The parameter  $f$  is the value of the reverse transmission—e.g., the  $y_{12}$  term of the two-port in Fig. 3(b). Measurement of  $f$  for the circuit in Fig. 2, ignoring dc bias, is shown in Fig. 5(a):  $f = y_{12} = i_{fb} / v_t$ . A general procedure for finding  $f$  for any type of feedback circuit at the closed-loop dc operating point is now

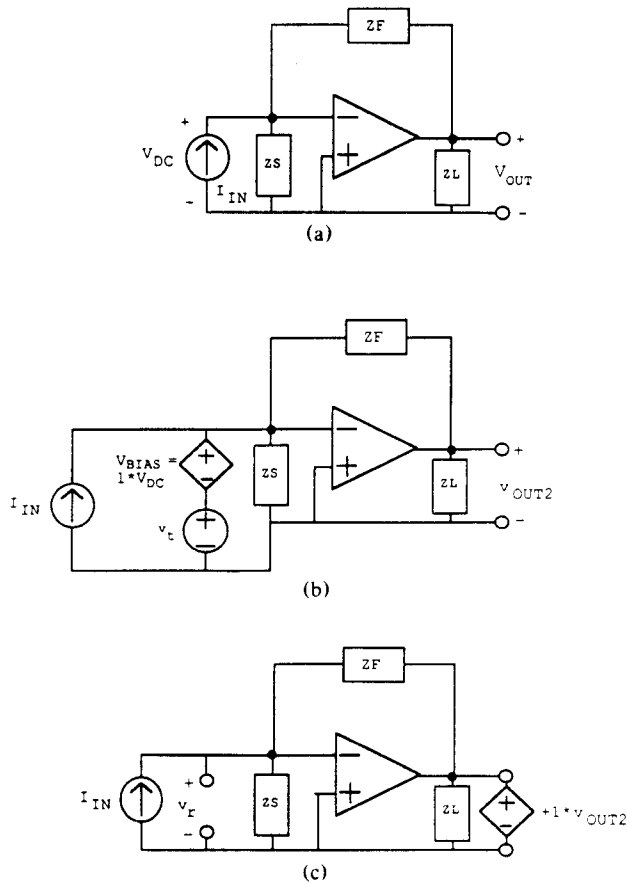


Fig. 6. Measurement of  $af = -G_1 \cdot G_2 = -v_t/v_r$  for the circuit in Fig. 2, including controlled sources to maintain the closed-loop dc operating point in (b) and (c). The dc reference circuit is (a).

presented. The ideas are to employ a dc reference circuit that is used to correctly set the operating point in the test circuit and to measure  $f$  by driving the output node of the closed-loop feedback circuit and measuring all reverse transmission into an ac short circuit or open circuit, depending upon the type of feedback. This two-step procedure is illustrated in Fig. 5(b) and (c) and is described next.

**Step 1:** Draw the feedback circuit, labeling the ac input source and output variable. The ac input source should be a current source if there is shunt feedback at the input, a voltage source for series feedback at the input. (Use Thevenin or Norton equivalents as required.) Make two copies of this circuit. In the first copy, if the ac input is a current (voltage) source, call the dc voltage (current) across (through) the input source  $V_{DC}$  ( $I_{DC}$ ). Now set the ac independent source to zero; this circuit will serve as the dc reference.

**Step 2:** In the second circuit, drive the output with a controlled source of the same type as the output variable, with value  $+1$  times the output of the first circuit. This controlled source is either a voltage-controlled voltage source or a current-controlled current source and will assure that the dc output biasing is correct. Connect in series (parallel) with this controlled voltage (current) source as independent ac voltage (current) source  $s_r$ . Also, replace the ac input source with an ideal meter of the same type and same polarity (i.e., replace a current source with an ideal ammeter (short circuit), or replace a voltage source with an ideal voltmeter (open circuit)). Call the measured quantity  $s_{fb}$ . Connect in series (parallel) with this ideal current

(voltage) meter a controlled voltage (current) source with value  $V_{BIAS} = 1 \cdot V_{DC}$  ( $I_{BIAS} = 1 \cdot I_{DC}$ ). (This source assures that the dc input biasing is correct.) The transfer function  $f = s_{fb}/s_r$  is the exact value of the reverse transmission evaluated at the closed-loop dc bias point.

#### 4.2. Simulating $af$

The loop gain  $af$  of Fig. 1(a) is a crucial parameter of a feedback circuit. Given the circuit topology and its input and output connections,  $af$  is uniquely defined. The loop-gain expression for shunt-shunt feedback was given in (6). A general procedure for finding  $af$  at the closed-loop dc operating point is now given and is illustrated in Fig. 6 for the shunt-shunt circuit in Fig. 2. The procedure is based on the observation that  $af$  can be broken into the cascade of two transfer functions:  $af = -G_1 \cdot G_2$  where, for the shunt-shunt case,  $G_1 = -y_{21}/y_{22}$  and  $G_2 = -y_{12}/y_{11}$ .  $G_1$  can be measured by driving the input port with a voltage source and measuring the output voltage.  $G_2$  can be measured by driving the output port with a voltage source and measuring the voltage across the input port. Therefore,  $af$  is measured by the two circuits in Fig. 6(b) and (c), which measure  $G_1$  and  $G_2$ , respectively. The general procedure for simulating  $af$  follows.

**Step 1:** Draw the feedback circuit, labeling the ac input source and output variable as in Step 1 above. Make three copies of this circuit. In the first copy, if the ac input is a current (voltage) source, call the dc voltage (current) across (through) the input source  $V_{DC}$  ( $I_{DC}$ ). Now set the ac independent source to zero; this circuit will serve as the dc reference.

**Step 2:** In the second circuit, replace the ac input current (voltage) source with an ac voltage (current) source. Call this new ac test source  $s_r$ . Connect in series (parallel) with  $s_r$  a controlled voltage (current) source with value  $V_{BIAS} = 1 \cdot V_{DC}$  ( $I_{BIAS} = 1 \cdot I_{DC}$ ). This controlled source will force the bias in the second circuit to match that of the dc reference circuit.

**Step 3:** In the third circuit, drive the output with a controlled source of the same type as the output variable, with value  $+1$  times the output of the second circuit. (This controlled source is either a current-controlled current source or a voltage-controlled voltage source.) Replace the ac input source with an ideal meter of the opposite type but the same polarity (i.e., a current source is replaced by an ideal voltmeter, a voltage source is replaced by an ideal ammeter). Call the measured value  $s_r$ . The transfer function  $af = -s_r/s_t$  is the exact value of the loop gain  $af$  evaluated at the closed-loop dc operating point.

In Fig. 6(b), the ac input source  $v_t$  drives the amplifier and the feedback circuit in the forward direction. This voltage drive at the summing node short circuits the feedback current, and therefore the output is  $v_o = -y_{21}v_t/y_{22}$ . Likewise, Fig. 6(c) measures only reverse transfer,<sup>3</sup> and as such  $af$  is being computed as

$$af = -\frac{v_r}{v_t} = -\frac{v_o}{v_t} \cdot \frac{v_r}{v_o} = -\frac{y_{21}}{y_{22}} \cdot \frac{y_{12}}{y_{11}} \quad (10)$$

The dc input sources and controlled sources assure that the proper dc biasing is maintained in the second and third circuits.

<sup>3</sup>A difficulty can arise if ideal amplifiers are employed. For instance, in Fig. 6(c), if the op-amp has zero output impedance, then two voltage sources would be connected together at the output node. This unrealistic situation can be avoided by adding a negligibly small output impedance to the op-amp.

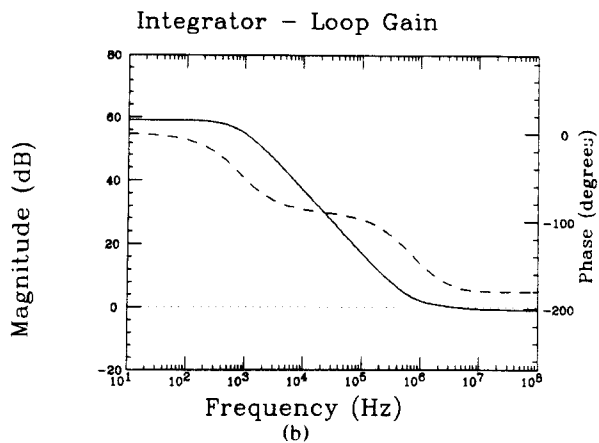
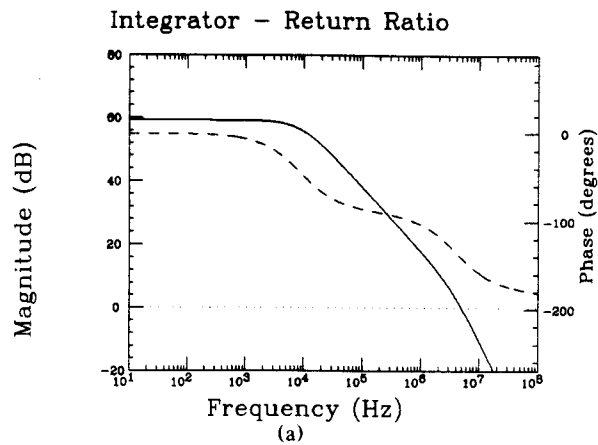


Fig. 7. Return ratio (a) and loop gain (b) simulation results for the circuit in Fig. 2 (phase is plotted with a dashed line) with component values  $Z_S = 1/(s \cdot 2 \text{ pF})$ ,  $Z_F = 1/(s \cdot 20 \text{ pF})$ ,  $Z_L = \infty \Omega$ . The op-amp model is  $Z_{in_a} = \infty \Omega$ ,  $Z_{out_a} = 10 \text{ M}\Omega$ , and  $a_i(s) = 1000/(1 + s/2.52e7)$ .

These techniques for finding  $f$  and  $af$  are exact. The usual approximations that simplify hand analysis (i.e., ignoring feedforward through the feedback network and ignoring reverse transmission through the amplifier) are not required here.

## V. EXAMPLES

Fig. 7 shows return-ratio and loop-gain plots for the circuit in Fig. 2 with capacitive feedback. (The element values are given in the caption of Fig. 7.) Differences are evident between the plots in Fig. 7: a) the loop-gain plot shows the effect of the feedforward zero due to the feedback capacitor, whereas the return-ratio plot is a two-pole response, and b) the  $-3\text{-dB}$  frequencies of the two plots are not the same. These plots again point out that, while both  $RR$  and  $af$  present useful information about the feedback loop, they are not equal in general.

An example of loop-gain simulation for a series-shunt feedback circuit is shown in Fig. 8. The loop-gain plot in Fig. 8(b)–(d) is produced by SPICE simulation of the test circuits shown in Fig. 8(b)–(d). Fig. 9 illustrates how the loop-gain simulation technique can be applied to a shunt-shunt feedback circuit that does not have a current source input. Only a Norton equivalence of the ac input is necessary; the dc input voltage source can remain intact for biasing. The loop-gain simulation procedure described above can be carried out, starting with Fig. 9(b).

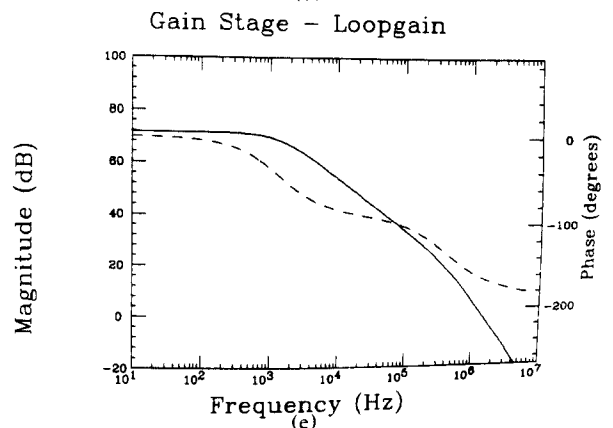
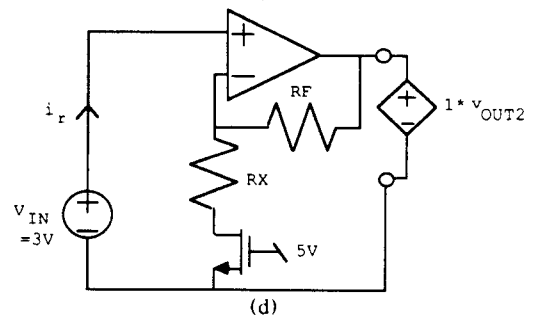
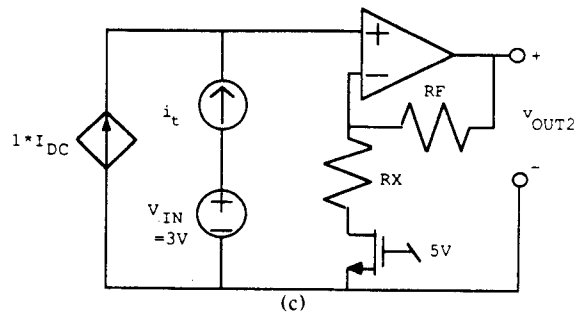
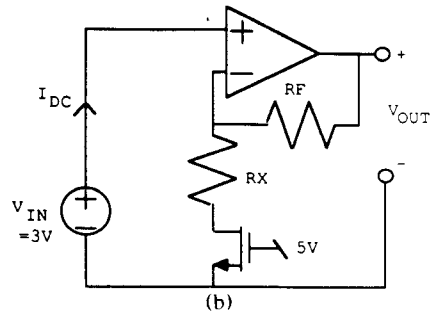
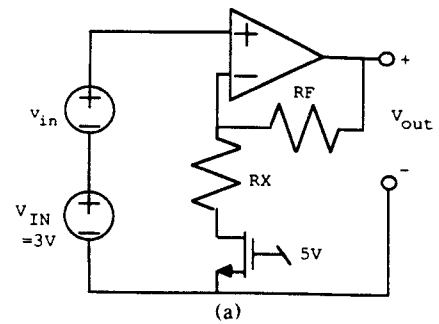


Fig. 8. (a) A series-shunt feedback circuit, and (b)–(d) the test circuits for loop gain simulation. The loop gain is plotted in (e). The phase is plotted as a dashed line. The op-amp has  $Z_{in_a} = 10 \text{ M}\Omega \parallel 2 \text{ pF}$ ,  $Z_{out_a} = 100 \Omega$ , and  $a_i(s) = 10000/(1 + s/8.6e3 + s/2.58e6)$ .  $R_F = 2 \text{ k}\Omega$ ,  $R_X = 1 \text{ k}\Omega$ , and the MOSFET switch is biased in the triode region with  $R_{on} = 300 \Omega$ .

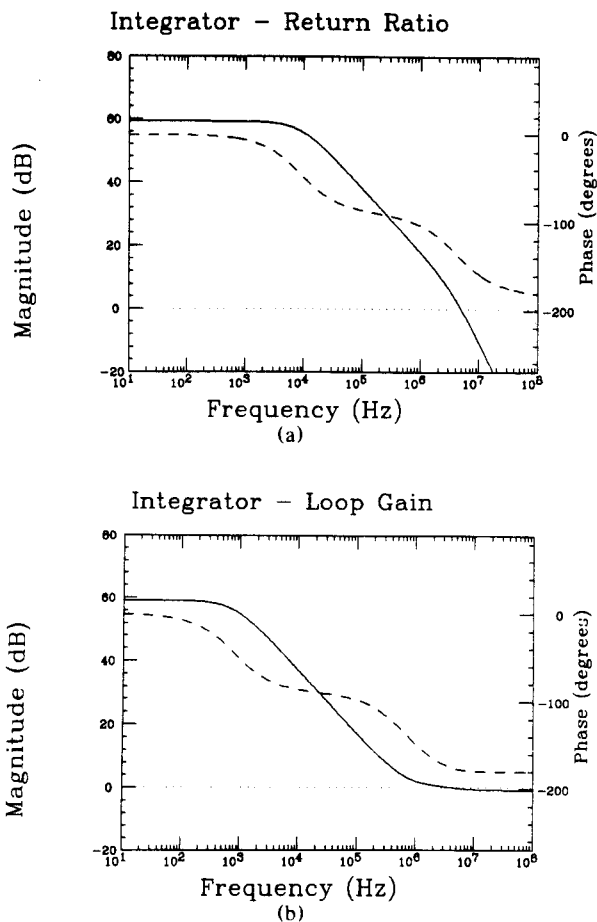


Fig. 7. Return ratio (a) and loop gain (b) simulation results for the circuit in Fig. 2 (phase is plotted with a dashed line) with component values  $Z_S = 1/(s \cdot 2 \text{ pF})$ ,  $Z_F = 1/(s \cdot 20 \text{ pF})$ ,  $Z_L = \infty \Omega$ . The op-amp model is  $Z_{in_a} = \infty \Omega$ ,  $Z_{out_a} = 10 \text{ M}\Omega$ , and  $a_f(s) = 1000/(1 + s/2.52e7)$ .

These techniques for finding  $f$  and  $af$  are exact. The usual approximations that simplify hand analysis (i.e., ignoring feedforward through the feedback network and ignoring reverse transmission through the amplifier) are not required here.

## V. EXAMPLES

Fig. 7 shows return-ratio and loop-gain plots for the circuit in Fig. 2 with capacitive feedback. (The element values are given in the caption of Fig. 7.) Differences are evident between the plots in Fig. 7: a) the loop-gain plot shows the effect of the feedforward zero due to the feedback capacitor, whereas the return-ratio plot is a two-pole response, and b) the  $-3$ -dB frequencies of the two plots are not the same. These plots again point out that, while both  $RR$  and  $af$  present useful information about the feedback loop, they are not equal in general.

An example of loop-gain simulation for a series-shunt feedback circuit is shown in Fig. 8. The loop-gain plot in Fig. 8 was produced by SPICE simulation of the test circuits shown in Fig. 8(b)–(d). Fig. 9 illustrates how the loop-gain simulation technique can be applied to a shunt-shunt feedback circuit that does not have a current source input. Only a Norton equivalence of the ac input is necessary; the dc input voltage source can remain intact for biasing. The loop-gain simulation procedure described above can be carried out, starting with Fig. 9(b).

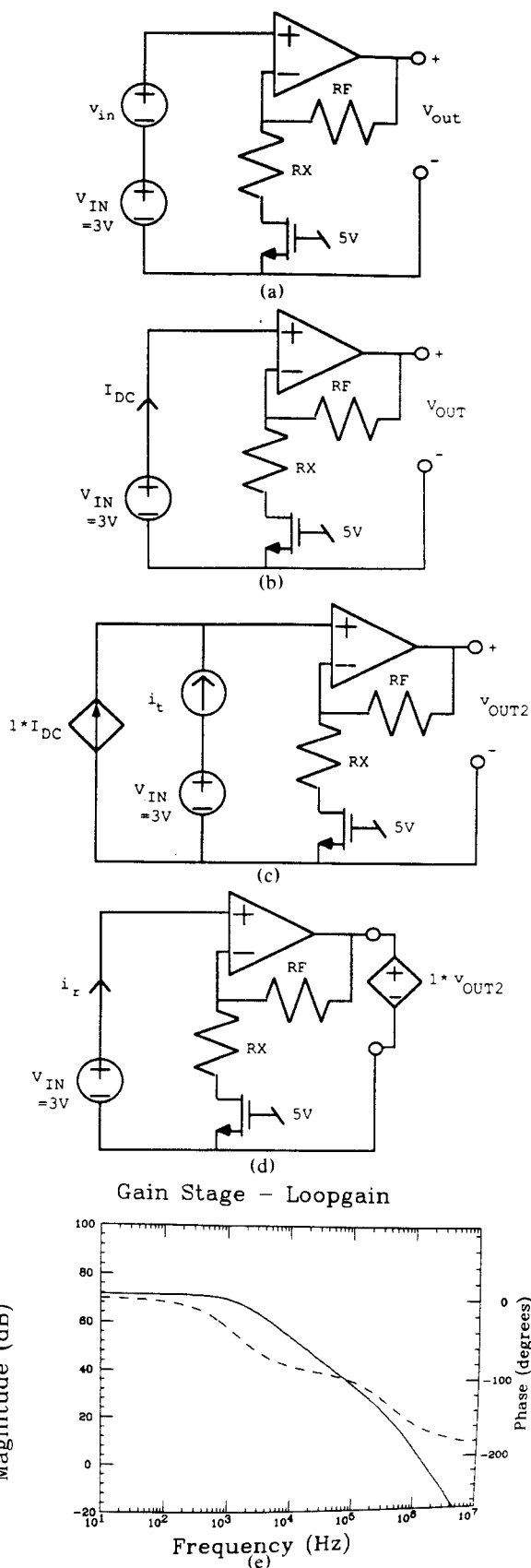


Fig. 8. (a) A series-shunt feedback circuit, and (b)–(d) the test circuits for loop gain simulation. The loop gain is plotted in (e). The phase is plotted as a dashed line. The op-amp has  $Z_{in_a} = 10 \text{ M}\Omega$ ,  $2 \text{ pF}$ ,  $Z_{out_a} = 100 \Omega$ , and  $a_f(s) = 10000/(1 + s/8.6e3)(1 + s/2.58e6)$ .  $R_F = 2 \text{ k}\Omega$ ,  $R_X = 1 \text{ k}\Omega$ , and the MOSFET switch is biased in the triode region with  $R_{on} = 300 \Omega$ .

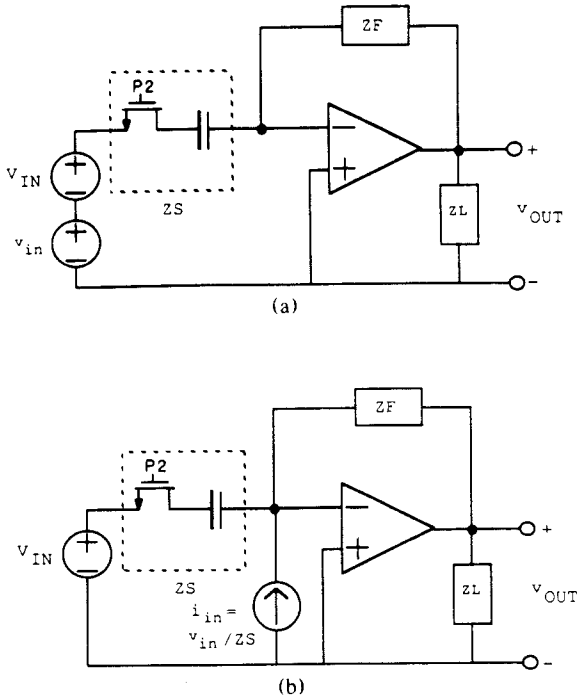


Fig. 9. (a) A shunt-shunt feedback circuit shown in the commonly used voltage gain configuration; (b) the same circuit after converting the ac input voltage to a current. The dc input voltage source remained in place, thereby assuring the proper biasing on the MOSFET switch.

The advantage of performing the feedback simulations at the closed-loop dc operating point can be emphasized by looking at these last two circuits. Simulation at the closed-loop dc operating point ensures accurate computation of the small-signal models for transistors in the op-amps, as well as for any nonlinear elements in the feedback network such as the MOSFET switches in Figs. 8 and 9.

The simulation methods for  $af$  and  $f$  require that the feedback circuit under test be of the form of two properly interconnected two-ports. While it is generally easy to visually determine from the schematic if the feedback network is a two-port, such a determination for the forward amplifier may be more difficult. An assumption that the forward amplifier can be modeled as a two-port can be tested during the simulations. For example, differences in the measured currents flowing into the op-amp inverting input and out of the noninverting input in Fig. 6(b) or Fig. 8(c) indicate that the op-amp cannot be modeled by a two-port.

## VI. RELATING RETURN RATIO TO LOOP GAIN $af^4$

Since the return ratio is clearly a measure of loop transmission, it should be possible to interpret it as a loop gain in some way. In fact, the return ratio for a controlled source is the same as the loop gain  $a'f'$  if the output variable is taken as the voltage across (current through) a controlled voltage (current) source and if the input source is a current source across the controlling voltage or a voltage source in series with the controlling current.<sup>5</sup> An example of such a circuit, with new output  $v'_{out}$ ,

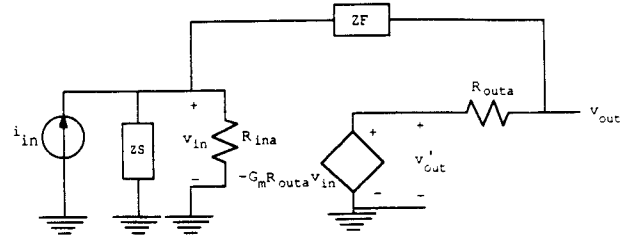


Fig. 10. A shunt-shunt feedback circuit (Fig. 2 redrawn) with the output  $i'_{out}$  taken across the VCVS.

is shown in Fig. 10. In such a case, the loop-gain simulation sends a signal from the controlled source back to the input port where the controlling signal is measured (Step 3 above) and then from the input port to the controlled source (Step 2 above). This simulation is essentially identical to a return-ratio computation (in two parts) for the controlled source, since an  $RR$  computation also sends a signal around the loop starting and ending at the controlled source.

There is an alternative way to prove this point. Under the conditions above, the direct feedthrough  $d$  is zero and  $b_2$  is unity. In addition, it can be shown that  $a = b_1 \cdot k$  (see below); therefore, the numerators of (2) and (3) are the same. Since (2) and (3) must give the same closed-loop gain, it follows that  $RR = a'f'$ .

To show that  $a = b_1 \cdot k$ , consider a shunt-shunt feedback circuit. Under the conditions above, the output  $v'_{out}$  must be directly across a voltage-controlled voltage source (VCVS), and the input is a current source driving the port across which the controlling voltage  $v_{in}$  is measured (e.g., Fig. 10). Therefore,  $v'_{out} = k \cdot v_{in}$ . With  $v'_{out}$  across a VCVS,  $y'_{21} = \infty \Omega^{-1}$  and  $y'_{22} = \infty \Omega^{-1}$ , but  $k = -y'_{21}/y'_{22}$  since  $v'_{out} = -y'_{21}v_{in}/y'_{22}$  is the Thevenin equivalent open-circuit voltage at the output in Fig. 3. Also,  $1/y'_{11} = v_{in}/i_{in}|_{v'_{out}=0V}$ , which is equivalent to  $b_1$  since  $b_1 = v_{in}/i_{in}|_{k=0} = v_{in}/i_{in}|_{v'_{out}=0V} = 1/y'_{11}$ . Therefore,  $a = -y'_{21}/y'_{22}y'_{11} = (-y'_{21}/y'_{22}) \cdot (1/y'_{11}) = k \cdot b_1$ .

For a sample calculation, consider Fig. 10, which is Fig. 2 redrawn. With the model of the op-amp in Thevenin form and the output of the feedback circuit across the VCVS,  $k = -G_m R_{outa} = -y'_{21}/y'_{22}$ . Now  $R_{outa}$  must be considered as part of the feedback network. Using the element values given in the caption of Fig. 2, the loop gain  $a'f'$  is

$$\begin{aligned} a'f' &= -\frac{(y'_{21a} + y'_{21f}) \cdot (y'_{12a} + y'_{12f})}{(y'_{11a} + y'_{11f}) \cdot (y'_{22a} + y'_{22f})} = -\frac{y'_{21}}{y'_{22}} \cdot \frac{(y'_{12a} + y'_{12f})}{(y'_{11a} + y'_{11f})} \\ &= (-G_m R_{outa}) \cdot \frac{(y'_{12a} + y'_{12f})}{(y'_{11a} + y'_{11f})} \\ &= (-10 \text{ m}\Omega^{-1} \cdot 1 \text{ M}\Omega) \\ &\quad \cdot \frac{\left( \frac{-1}{100 \text{ k}\Omega + 1 \text{ M}\Omega} \right)}{\left( \frac{1}{500 \text{ k}\Omega} + \frac{1}{1 \text{ M}\Omega} + \frac{1}{100 \text{ k}\Omega + 1 \text{ M}\Omega} \right)} = 2326. \quad (11) \end{aligned}$$

This  $a'f'$  is identical to the return ratio computed in (8). (Although not included here, a shunt-series analysis using  $g$ -parameters with the output equal to the current out of the  $G_m$  controlled source gives  $a''f'' = 2326$ .)

<sup>4</sup>Further discussion on this topic can be found in [12].

<sup>5</sup>If there are multiple dependent sources, the output can be taken from any dependent source and the input can be placed across any of the controlling signals.



Since  $RR$  corresponds to  $af$  for some input/output pair,  $RR$  can be used to check stability and predict closed-loop performance for the corresponding transfer function. Since the poles of the transfer function depend on the network, not on the specific input and output chosen (unless the particular transfer function happens to introduce a zero that cancels a pole), using  $RR$  rather than the correct  $af$  to check the stability of any transfer function is acceptable, but simulation of the correct loop gain is preferred.

## VII. CONCLUSION

Systematic techniques for performing computer simulation of single-loop feedback circuit parameters have been presented. The techniques can be used by analog circuit designers and may find applications in automated analog design software. The results of the computer simulations are exact; no simplifying approximations are necessary. The practical difficulty of maintaining the proper dc operating point while measuring the loop parameters of the feedback circuit has been solved by using controlled sources and a dc reference circuit. This allows the circuit simulation program to accurately compute the linear small-signal equivalent for all nonlinear elements in the feedback loop. These techniques are particularly useful for handling complex feedback circuits with nonlinear elements.

As background, discussions of return-ratio-based and classical feedback circuit analysis were included with an example that clearly shows that  $RR$  and  $af$  can be quite different. Also, an interpretation of return ratio as the loop gain of an appropriately defined transfer function has been presented.

These simulation methods were illustrated by two examples and have been used successfully on more than a dozen other CMOS shunt-shunt feedback circuit designs employing op-amps. The methods use frequency-domain analysis, which is preferred over transient analysis since the former requires much less computation and is therefore much faster than the latter, although some transient simulations must be run to check slew rate and to verify the settling time.

## ACKNOWLEDGMENT

The author gratefully acknowledges the comments of Stephen Lewis and the verification of these simulation techniques by William Alexander III, H. Greg Bell, David Block, James Brown, Edward Lemos, Roger Levinson, and William McIntyre.

## REFERENCES

- [1] P. R. Gray and R. G. Meyer, *Analysis and Design of Analog Integrated Circuits*. New York: Wiley, 1984.
- [2] A. S. Sedra and K. C. Smith, *Microelectronic Circuits*. New York: Holt, Rinehart, and Winston, 1987.
- [3] P. E. Gray and C. L. Searle, *Electronic Principles: Physics, Models, and Circuits*. New York: Wiley, 1969.
- [4] H. W. Bode, *Network Analysis and Feedback Amplifier Design*. New York: Van Nostrand, 1945.
- [5] E. S. Kuh and R. A. Rohrer, *Theory of Linear Active Networks*. San Francisco, CA: Holden-Day, 1967.
- [6] S. Rosenstark, *Feedback Amplifier Principles*. New York: MacMillan, 1986.
- [7] S. S. Hakim, *Feedback Circuit Analysis*. New York: Wiley, 1966.
- [8] C. A. Holt, *Electronic Circuits—Digital and Analog*. New York: Wiley, 1978.
- [9] D. Casasent, *Electronic Circuits*. New York: Quantum, 1973.
- [10] S. Rosenstark, "Loop gain measurement in feedback amplifiers," *Int. J. Electron.*, vol. 57, pp. 415-421, 1984.

- [11] R. D. Middlebrook, "Measurement of loop gain in feedback systems," *Int. J. Electron.*, vol. 38, pp. 485-512, 1975.
- [12] P. J. Hurst, "A comparison of two approaches to feedback circuit analysis," submitted for publication in *IEEE Trans. Education*, 1992.

## A Bound Involving $n$ -Dimensional Instantaneous Frequency

Alan C. Bovik

We state and prove an integral inequality that bounds the absolute difference

$$\epsilon(\mathbf{x}) = |m(\mathbf{x}) - \hat{m}(\mathbf{x})| \quad (1)$$

where

$$m(\mathbf{x}) = |w(\mathbf{x}) \exp(j\mathbf{x}^T \mathbf{u}_0) * \exp[ju(\mathbf{x})]| \quad (2)$$

is the response of a modulated  $n$ -dimensional real linear filter  $w$  to a complex exponential signal with  $n$ -dimensional instantaneous frequency  $\nabla u(\mathbf{x})$ , and where

$$\hat{m}(\mathbf{x}) = |W[\nabla u(\mathbf{x}) - \mathbf{u}_0]| \quad (3)$$

where  $W$  is the Fourier transform of  $w$ . The quantity  $\epsilon(\mathbf{x})$  provides an estimate of the error incurred by using  $\hat{m}(\mathbf{x})$  as an estimate of  $m(\mathbf{x})$ , e.g., if  $\nabla u(\mathbf{x})$  is unknown. Such estimates may be applied to the problem of measuring the  $n$ -dimensional instantaneous frequency of nonstationary phase-modulated signals of the form  $\exp[ju(\mathbf{x})]$ , by solving  $\nabla u(\mathbf{x})$  in terms of the known modulation frequency  $\mathbf{u}_0$  and the known filter  $w$ , possibly subject to additional constraints such as smoothness of  $\nabla u(\mathbf{x})$ . In fact, the bound is expressed in terms of a smoothness functional (Sobolev norm) of  $\nabla u(\mathbf{x})$  and a generalized measure of the localization (duration) of  $w$ . Such signals occur in a variety of multidimensional system applications, such as audio signal recognition or composition, and in the analysis of patterned images.

We denote points in  $\mathbf{R}^n$  by  $\mathbf{t} = (t_1, t_2, \dots, t_n)$ ,  $d\mathbf{t} = dt_1 dt_2 \dots dt_n$ , and the partial derivatives of  $u: \mathbf{R}^n \rightarrow \mathbf{R}$  twice-differentiable at  $\mathbf{t}$  by  $\partial^2 / (\partial t_i \partial t_j) u(\mathbf{t}) = u^{(i,j)}(\mathbf{t})$ , unless  $n = 1$ , in which case  $\partial^2 / (\partial t^2) u(\mathbf{t}) = u''(\mathbf{t})$ .

*Theorem:* Let  $w: \mathbf{R}^n \rightarrow \mathbf{R}$  be any function for which  $|t_i t_j w(\mathbf{t})|^p$  is integrable on  $\mathbf{R}^n$  for  $i, j = 1, \dots, n$ , and let  $u: \mathbf{R}^n \rightarrow \mathbf{R}$  be any twice-differentiable function for which  $|u^{(i,j)}(\mathbf{t})|^q$  is integrable on  $\mathbf{R}^n$  for  $i, j = 1, \dots, n$ , where  $q > n$  and  $(1/p) + (1/q) = 1$ . If  $\epsilon(\mathbf{x})$  is given by (1)–(3), then

$$\epsilon(\mathbf{x}) \leq \frac{q^2}{(q-n)(2q-n)} \left[ \sum_{i=1}^n \sum_{j=1}^n \int_{\mathbf{R}^n} |t_i t_j|^p |w(\mathbf{t})|^p d\mathbf{t} \right]^{\frac{1}{p}} \cdot \left[ \sum_{i=1}^n \sum_{j=1}^n \int_{\mathbf{R}^n} |u^{(i,j)}(\mathbf{t})|^q d\mathbf{t} \right]^{\frac{1}{q}}. \quad (4)$$

Manuscript received January 25, 1991; revised May 6, 1991. This paper was recommended by Associate Editor Y. F. Huang.

The author is with the Department of Electrical and Computer Engineering, University of Texas, Austin, TX 78712-1084.

IEEE Log Number 9102891.